The role of the Roper resonance in $np \to d(\pi\pi)^0$

L. Alvarez-Ruso

Departamento de Física Teórica and IFIC, Centro Mixto Universidad de Valencia-CSIC, 46100 Burjassot, Valencia, Spain

Abstract

In this work, a model for the $np \to d(\pi\pi)^0$ reaction is developed. It is shown that the structure of the deuteron momentum spectra for a neutron beam momentum of 1.46 GeV can be explained as a consequence of the interplay of two mechanisms involving the excitation of the $N^*(1440)$ resonance and its subsequent decay into $N(\pi\pi)^{T=0}_{S-wave}$ and $\Delta\pi$ respectively. The relevance of the present analysis for the study of the Roper excitation and decay properties, as well as for the interpretation of other two-pion production experiments is discussed.

1 Introduction

The study of nucleon-nucleon inelastic collisions provides a powerful tool to deepen our insight into the properties of nucleon-nucleon interactions and baryonic resonances. A large amount of theoretical work on threshold meson production has been performed over the last years [1], stimulated by the precise data obtained at IUCF, CELSIUS and COSY [2]. On the other side, double pion production reactions in the nucleon, $\gamma N \to N\pi\pi$ and $\pi N \to N\pi\pi$, have proved to be essential as a test of Chiral Perturbation Theory [3] and as a source of information about $N^*(1440)$ and $N^*(1520)$ [4–7]. In this context, the still scantily explored two pion production channel in the collisions of nucleons and light nuclei appears as promising research area.

Most of the work, both experimental and theoretical, on two pion production in nucleon-nucleon collisions was performed in the seventies and in connection with the ABC effect. The ABC anomaly is an enhancement in the missing mass spectra close to the $\pi\pi$ production threshold, observed for the reactions $pd \to {}^3HeX$ [8], $np \to dX$ [9] and $dd \to {}^4HeX$ [10]. Although any interpretation of the ABC as a resonance is excluded [9], the origin of it is still poorly understood [9,11]. An important step towards the understanding of the ABC effect has

been taken in Ref. [12], where the ^4He spectra from the $dd \to {}^4HeX$ reaction at a deuteron beam energy of 1250 MeV [10] has been explained assuming that pions are independently produced in reactions involving two different pairs of nucleons from the projectile and target deuterons. Nowadays, two pion production in pp collisions is being studied experimentally at CELSIUS for beam kinetic energies between 650 and 775 MeV. On the theoretical side, a microscopic model for the $NN \to NN\pi\pi$ reaction has been recently developed [13]. It includes mechanisms with the excitation of N^* and Δ resonances, as well as some non-resonant contributions, and gives a satisfactory description of the available experimental data on total cross sections for most of the channels and in a wide range of energies up to 800 MeV above threshold.

In this letter, I focus the attention on the deuteron spectrum in $np \to d(\pi\pi)^0$ measured by Hollas and collaborators [14] using a nearly monokinetic neutron beam with central momentum $p_n = 1.463$ GeV. This experiment is somewhat similar to the one of Plouin et al. [9], but at lower energies ($T_n = 795$ MeV in [14] vs 1160 MeV in [9]). Therefore, the analysis is simpler since, once the π^0 peaks are subtracted, only the double pion production mechanism is present. Apart from that, one expects that, being closer to threshold, the reaction mechanism might be simpler. The ABC peaks are not present in the data; they rather show a well defined bump at high $\pi\pi$ missing masses, in disagreement with the models available in the literature [15,16]. From this comparison, the authors concluded [14] that neither double-Δ formation nor double-nucleon exchange provides the appropriate description of the reaction at $p_n = 1.46$ GeV. A similar enhancement has also been observed for the reaction $pd \to {}^3He\pi^+\pi^-$, which is being studied using a beam of protons from COSY (MOMO experiment) [17], at a Q value close to the one of the experiment by Hollas et al. [14]. These common features point to a common dynamical description.

Here, it is shown that the deuteron spectra for $np \to d(\pi\pi)^0$ at $p_n = 1.46$ GeV can be understood as a consequence of the interference of two mechanisms involving the excitation of the Roper resonance $N^*(1440)$ and its subsequent decay into $N(\pi\pi)^{T=0}_{S-wave}$ and $\Delta\pi$ respectively. The implications of this finding to the MOMO experiment are also discussed.

2 The model

The model is schematically presented in Fig. 1. It is a reduced version of the model of Ref. [13], modified for the case where one has a deuteron instead of two free nucleons in the final state. The choice of the mechanisms was based on their contribution to the total cross section for the $pn \to pn\pi^+\pi^-$ reaction; the situation for the $pn \to pn\pi^0\pi^0$ channel is similar. At $T_p = 800$ MeV,

the mechanism with $N^* \to N(\pi\pi)^{T=0}_{S-wave}$ gives $\sigma \sim 11\,\mu b$, being by far the most important. The second largest contribution comes from $N^* \to \Delta\pi$ with $\sigma \sim 0.5\,\mu b$; as we will see, in the case of a deuteron in the final state, its contribution is larger with respect to the dominant $N^* \to N(\pi\pi)^{T=0}_{S-wave}$ and crucial to obtain the right shape. All other mechanisms give $\sigma \lesssim 0.3\,\mu b$; I do not include them all, but just the double-Δ ($\sigma \sim 0.1\,\mu b$) one in order to make contact with the model of Ref. [16].

The deuteron momentum spectrum is the sum of the $\pi^+\pi^-$ and the $\pi^0\pi^0$ contributions. In the Laboratory frame, the charged pions piece is given by

$$\frac{d^2\sigma}{dp'_d d\Omega'_d} = \frac{1}{4}\frac{1}{(2\pi)^5}\frac{M M_d (p'_d)^2}{E'_d p_n p_d}\left(\int dE_\pi d\varphi_\pi \frac{1}{4}\sum_{Rr_1r_2}|\mathcal{M}_{Rr_1r_2}|^2\right)_{CM} . \quad (1)$$

Here, E'_d and p'_d are the deuteron energy and the modulus of its momentum, both in Lab. frame; p_d is the modulus of the deuteron momentum in the center-of-mass system (CM); M and M_d stand for the nucleon and deuteron masses respectively. The integral in brackets must be calculated with all the kinematical variables defined in CM; it runs over the polar angle and the energy of one of the outgoing pions. The amplitude squared is summed over the deuteron spin (R) and averaged over the spins of the incoming nucleons (r_1, r_2). For the neutral pions channel, the expression is the same but with and extra 1/2 factor, which is a consequence of having two identical pions in the final state. The difference of masses between charged and neutral pions is taken into account for the phase space, but isospin symmetry is assumed in the calculation of the amplitude.

The amplitude can be expressed as

$$\mathcal{M}_{Rr_1r_2} = \sum_{r'_1 r'_2}\left(\frac{1}{2}r'_1\frac{1}{2}r'_2\right| 1R\Big) \int \frac{d\mathbf{q}}{(2\pi)^3} D_{T=0,1}(q) \times$$

$$\Big\{\Big(\langle pr'_1|\,\hat{V}_1\,|pr_1\rangle\,\langle nr'_2|\,\hat{V}_2\,|nr_2\rangle - \langle nr'_1|\,\hat{V}_1\,|pr_1\rangle\,\langle pr'_2|\,\hat{V}_2\,|nr_2\rangle\Big)\,\tilde{\varphi}_d(\mathbf{P_2})$$

$$+\Big(\langle pr'_1|\,\hat{V}_2\,|pr_1\rangle\,\langle nr'_2|\,\hat{V}_1\,|nr_2\rangle - \langle nr'_1|\,\hat{V}_2\,|pr_1\rangle\,\langle pr'_2|\,\hat{V}_1\,|nr_2\rangle\Big)\,\tilde{\varphi}_d(\mathbf{P_1})\Big\} \quad (2)$$

where $\tilde{\varphi}_d(\mathbf{P})$ is the s-wave deuteron wave function in momentum space, normalized as

$$\int \frac{d\mathbf{k}}{(2\pi)^3}\,\tilde{\varphi}_d^2(\mathbf{k}) = 1. \quad (3)$$

The d-wave part has been neglected. For the wave function, different expres-

sions and parameterizations can be used [18–20]. The value of $\mathbf{P_{1(2)}}$ depends on the mechanism; for those of Figs. 1a and 1b, $\mathbf{P_{1(2)}} = \mathbf{q} + \mathbf{p_{1(2)}} - \mathbf{p_d}/2$ and for the $\Delta - \Delta$ mechanism (Fig. 1c) $\mathbf{P_{1(2)}} = \mathbf{q} + \mathbf{p_{1(2)}} - \mathbf{p_d}/2 - \mathbf{p_\pi}$, $\mathbf{p_{1(2)}}$ and $\mathbf{p_d}$ been the momenta of the proton (neutron) and deuteron respectively; $\mathbf{p_\pi}$ is the momentum of the pion, over whose energy the integral in Eq. 1 is performed. The function $D_{T=0,1}(q)$, which stands for the meson propagators and form factors, will be discussed later; $q = (q_0, \mathbf{q})$ is the four momentum transfer from one nucleon to the other; q_0 is given by energy conservation in the vertices and, therefore, depends on the energy of one of the outgoing nucleons, taken to be one half of the deuteron energy.

The matrix elements in Eq. 2 are evaluated for the different mechanisms using the Feynman rules that can be obtained using phenomenological Lagrangians; some of the required ones are

$$\mathcal{L}_{\Delta N\pi} = \frac{f^*}{m_\pi}\psi^\dagger_\Delta S^\dagger_i(\partial_i\boldsymbol{\phi})\mathbf{T}^\dagger\psi_N \; + \; h.c.\,, \tag{4}$$

$$\mathcal{L}_{N^*N\pi} = \frac{\tilde{f}}{m_\pi}\psi^\dagger_{N^*}\sigma_i(\partial_i\boldsymbol{\phi})\boldsymbol{\tau}\psi_N \; + \; h.c.\,, \tag{5}$$

$$\mathcal{L}_{N^*\Delta\pi} = \frac{g_{N^*\Delta\pi}}{m_\pi}\psi^\dagger_\Delta S^\dagger_i(\partial_i\boldsymbol{\phi})\mathbf{T}^\dagger\psi_{N^*} \; + \; h.c.\,. \tag{6}$$

In Eqs. 4, 6, $\mathbf{S}^\dagger$ ($\mathbf{T}^\dagger$) are the spin (isospin) $1/2 \to 3/2$ transition operators [21]; ψ_N, ψ_Δ, ψ_{N^*} and $\boldsymbol{\phi}$ stand for the nucleon, Delta, Roper and pion fields, while m_π is the pion mass. The absolute value of the coupling constants $f^* = 2.13$, $\tilde{f} = 0.477$ and $g_{N^*\Delta\pi} = 2.07$ are obtained from the partial decay widths of the Δ and $N^*(1440)$ [22]. In the case of the decays $N^* \to N\pi$ and $N^* \to \Delta\pi$, branching ratios of 65% and 25% respectively are assumed, as well as an N^* total width of 350 MeV; the signs correspond to those provided in earlier analyses of the $(\pi, \pi\pi)$ reactions [5,6]. The Lagrangian for the $NN\pi$ vertex is the standard one which, in the non-relativistic limit, looks like

$$\mathcal{L}_{NN\pi} = \frac{f_{NN\pi}}{m_\pi}\psi^\dagger_N\sigma_i(\partial_i\boldsymbol{\phi})\boldsymbol{\tau}\psi_N\,, \tag{7}$$

with $f_{NN\pi} = 1$.

A general Lagrangian for the $N^* \to N(\pi\pi)^{T=0}_{S-wave}$ decay [23] is

$$\begin{aligned}\mathcal{L}_{N^*N\pi\pi} = & - c_1^*\frac{m_\pi^2}{f^2}\bar{\psi}_{N^*}\boldsymbol{\phi}^2\psi_N \\ & - c_2^*\frac{1}{f^2 M^{*2}}(\partial_\mu\partial_\nu\bar{\psi}_{N^*})(\boldsymbol{\tau}\partial_\mu\boldsymbol{\phi})(\boldsymbol{\tau}\partial_\nu\boldsymbol{\phi})\psi_N \; + \; h.c.\end{aligned} \tag{8}$$

where $f = 92.4$ MeV is the pion decay constant and M^*, the mass of the Roper resonance. Using the partial decay width, the parameters c_1^* and c_2^* can be constrained to an ellipse [23]. In order to further constrain them, the model of Ref. [6] and the overall data on $\pi^- p \to \pi^+\pi^- n$ have been used [24]. Assuming a branching ratio of 7.5% for the $N^* \to N(\pi\pi)^{T=0}_{S-wave}$ decay, the best agreement is obtained for $c_1^* = -7.3$ GeV^{-1} and $c_2^* = 0$ (Set I), but the data seem to be still compatible with the choice of $c_1^* = -12.7$ GeV^{-1} and $c_2^* = 2.0$ GeV^{-1} (Set II). In this study, Set I will be used except where a different choice is explicitly indicated.

The matrix elements of Eq. 2 contain, apart from the vertices described above, Roper and Delta propagators, given by

$$D_l(p) = \frac{1}{\sqrt{p^2} - M_l + \frac{1}{2} i\Gamma_l(p)} \frac{M_l}{\sqrt{M_l^2 + \mathbf{p}_l^2}} \quad ; \qquad l = (N^*, \Delta) \tag{9}$$

with $p = (p_0, \mathbf{p})$ the momentum of the resonance and $\Gamma_l(p)$, its total width. The partial decay $\Delta \to N\pi$ practically accounts for the total Delta width. In the case of the Roper, the major part of the width comes from the decay into nucleon and pion and the rest from the decay into nucleon and two pions. All of them, except the small (less than 8% at the N^* peak) $N^* \to N\rho$ decay, can be calculated with the Lagrangians given above.

Finally, let us consider $D_{T=0,1}(q)$. For the $T = 1$ potential, I calculate the diagrams assuming a pion exchange and make the substitution

$$D^{(\pi)}_{T=1}(q) q_i q_j \to V'_L(q) \hat{q}_i \hat{q}_j + V'_T(q)(\delta_{ij} - \hat{q}_i \hat{q}_j) \tag{10}$$

so that $D_{T=1}$ includes the longitudinal pion exchange, the transversal rho exchange, and the short range correlations that take into account the repulsive force at short distances. Functions $V'_L(q)$ and $V'_T(q)$ are described elsewhere [13,25]. With respect to the $T = 0$ channel, in a recent analysis [26] of the (α, α') reaction on a proton target, the strength of the isoscalar $NN \to NN^*$ transition was extracted by parameterizing the transition amplitude in terms of an effective "σ" which couples to NN as the Bonn model σ ($g^2_{\sigma NN}/4\pi = 5.69$) [19] and couples to NN^* with an unknown strength provided by a best fit to the data ($g^2_{\sigma NN^*}/4\pi = 1.33$). According to the fit, $g_{\sigma NN}$ and $g_{\sigma NN^*}$ have the same sign. Therefore, we have

$$D_{T=0}(q) = \frac{1}{q^2 - m_\sigma^2} \left(\frac{\Lambda_\sigma^2 - m_\sigma^2}{\Lambda_\sigma^2 - q^2} \right)^2 , \tag{11}$$

where an equal $\Lambda_\sigma = 1.7$ GeV for the form factor is assumed for both vertices. The explicit expressions for the amplitudes are too involved to be reproduced

here, but some details of their evaluation can be traced in Ref. [13], where all the amplitudes for the free reaction $pp \to pp\pi^+\pi^-$ are given in the Appendix.

3 Results and discussion

With the ingredients described in the previous section, one can calculate the deuteron spectra at $p_n = 1.46$ GeV for different angles. The results are shown in Fig. 2. They compare quite well with the data of Hollas et al. [14], and certainly much better than the previous models [15,16]. The curves, in general, underestimate the data, maybe because there are many other mechanisms, not considered for the sake of simplicity, that, even been individually small, could in sum enhance the cross section. Some of the approximations made, like the neglect of the deuteron d-wave and non-relativistic approximation in the vertices, as well as the intrinsic uncertainties of the mechanisms included can also be a source of discrepancies; they are discussed below. The large data point at the edges of the spectra show the contamination of the π^0 peaks [14]. I have also estimated the influence of the width of the neutron beam by averaging the double differential cross sections over a Breit-Wigner profile of 40 MeV width and centered at $p_n = 1.46$ GeV [14]; the contribution of this effect is very small and irrelevant for our study. The plotted curves are obtained using the deuteron wave function derived from the Paris potential [18]; with the Bonn wave functions [19] the results are very similar, while for the Hulthen one [20] the distributions are overall larger, up to a factor two at the position of the central bump.

The mechanism $N^* \to N(\pi\pi)^{T=0}_{S-wave}$ (Fig. 1a) produces spectra very similar to phase space; its contribution is certainly the largest, but its relative size with respect to the $N^* \to \Delta\pi$ mechanism is not as large as one would naively expect from estimations based on the total cross sections obtained for both mechanisms in the free $NN \to NN\pi\pi$ reaction. Nevertheless, it is not surprising since here we are sensitive only to a reduced phase space region and choosing a particular combination of the quantum numbers of the outgoing nucleons (those of the deuteron). For this mechanism, I have calculated the contribution of the d-wave part of the deuteron wave function and found it negligible.

The $N^* \to \Delta\pi$ mechanism (Fig. 1b) exhibits a wide bump at the center of the spectra (high $\pi\pi$ masses), whose maximum falls fast with the increase of the deuteron angle, and small peaks at the edges of the spectra (low $\pi\pi$ masses); the size of these peaks does not vary appreciably with the angle. This mechanism plays a crucial role in providing the right shape to the distributions through its interference with the larger $NN \to NN\pi\pi$ contribution. This interference is constructive at high $\pi\pi$ masses and destructive at low ones.

Such pattern can be understood by realizing that the $N^* \to \Delta\pi$ amplitude is dominated by terms proportional to the scalar product of the outgoing pions three momenta; this scalar product has different signs in the center of the spectra, where the pions go back to back, and at the edges, where they travel together. In order to further illustrate the effect of the interference, Fig. 3 shows the effect of changing the relative sign of the two amplitudes. The data clearly favor a choice of the sign of $g_{N^*\Delta\pi}$ in agreement with earlier works [5,6].

The double-Δ mechanism (Fig. 1) is so small that it can hardly be distinguished in Fig. 2. In Fig. 4, the contribution of this mechanism alone is shown for $p_n = 1.5$ GeV, $\theta_{lab} = 4.5^\circ$ and using the Hulthen wave function, in order to compare with the result of Bar-Nir, Risser and Shuster (Fig. 4 b of Ref. [16]). The differential cross section obtained in the case of only pion exchange is very similar to the one given by the relativistic model of Ref. [16]; the inclusion of the rho exchange modifies the result, and the short range correlations between the initial nucleons cause a strong reduction of the strength of this mechanism. At $T_p = 775$ MeV ($p_p = 1.43$ GeV), the $pp \to pn\pi\pi$ and $pp \to d\pi\pi$ reactions are probably dominated by the double-Δ mechanism; therefore, the future data from CELSIUS would provide an excellent opportunity to study the interplay of the described ingredients and, in particular, the role of the short range correlations.

Wherever dealing with the Roper resonance, the lack of a precise determination of its properties is a problem that should be faced. In Fig. 5, I investigate how the results vary with some of the uncertainties. As can be noticed, the shape is not affected by these changes, but some set of values are preferred. Fig. 5 a, shows how the spectrum changes with the modification of c_1^*, c_2^* within the previously accepted values, while keeping the total width and the partial branching ratios fixed; set II gives a better agreement with the data. In Fig 5 b, we show the range of uncertainties that come from the variation of the total width of the N^* in the limits given by the Particle Data Book [22], that is from 250 MeV (lower line) to 450 MeV (upper line). Finally, the dependence on the partial branchings of the N^* to $N(\pi\pi)^{T=0}_{S-wave}$ and $\Delta\pi$, with the total width fixed to 350 MeV, is studied in Fig. 5 c. The dashed line corresponds to a 5% branching of N^* to $N(\pi\pi)^{T=0}_{S-wave}$ and a 30% to $\Delta\pi$, while for the dash-dotted one, a larger 10% of $N(\pi\pi)^{T=0}_{S-wave}$ and a smaller 20% of $\Delta\pi$; the data prefer the latter choice. These data alone do not allow to disentangle the different effects, but, in combination with other data that will be available in the future (like the data on $pp \to d\pi\pi$ at $T_p = 600 - 775$ MeV from CELSIUS), would be an important source of information about the Roper resonance.

As mentioned in the Introduction, the present model could provide an explanation to the deviation from phase space observed in the two pion invariant mass distribution of the reaction $pd \to {}^3He\pi^+\pi^-$, studied with a proton beam of momentum $p_p = 1.15$ GeV [17]. This experimental result has been inter-

preted with the hypothesis that the pions are preferably emitted in p-wave [27]. An ansatz based on this idea can explain the data reasonably well but, unfortunately, the initial tail of the ρ meson produced via $pd \to {}^3He\rho$ can hardly produce the required strength. In Fig. 6, we show the same observable for the reaction $np \to d\pi\pi$; the shape obtained for the charged pions channel is very similar to the one observed at COSY. The neutral pion channel, though, exhibits a shape similar to the one of the charged pions, and only a factor about 1/2 smaller at the peak position, in apparent contradiction with the much smaller rate of π^0 pairs, compared to the charged ones, obtained in the MOMO experiment. This is a consequence of the fact that, in the present model, the pions are almost always produced in s-wave. However, we should bear in mind that the interference pattern can be very different when the nucleons are bound in a ${}^3He$ nucleus instead of a deuteron. Detailed calculations are, therefore, required to check if the model can explain the MOMO experiment.

4 Conclusions

In summary, a simple model for the $np \to d(\pi\pi)^0$ reaction has been developed, based on a previous model for the free $NN \to NN\pi\pi$ and including the most important resonance contributions. It is shown that the bump in the center of the deuteron momentum spectra (high $\pi\pi$ masses) observed at a neutron beam momentum of $p_n = 1.463$ GeV ($T_p = 795$ MeV) can be explained as a result of the interference of two mechanisms involving the excitation of the Roper resonance: the dominant and phase-space like $N^* \to N(\pi\pi)^{T=0}_{S-wave}$ (Fig. 1 a) and the smaller in size $N^* \to \Delta\pi$ (Fig. 1 b), but determinant to obtain the right profile. The mechanism of double-Δ (Fig. 1 c) excitation, considered in an earlier model for the same reaction, but only including pion exchange, is significantly reduced by the short range correlations. Other two pion production reactions like $pp \to pn\pi\pi$ and $pp \to d\pi\pi$, currently studied experimentally at CELSIUS for energies between 650 and 775 MeV, would be helpful to clarify this issue, The size of the spectra depends appreciably on the Roper resonance and can be used, together with other two pion production reactions, to learn more about this resonance and its decay properties. Finally, the present model could be helpful to understand the two-pion invariant mass distributions observed from $pd \to {}^3He\pi^+\pi^-$ at COSY.

Acknowledgements

The author is indebted to C. Wilkin for drawing his attention to the work of Hollas and collaborators and its connection with the MOMO experiment. He has greatly benefited from discussions with E. Hernández, E. Oset and M. J. Vicente Vacas. He is also grateful to G. Faldt for his hospitality at TSL, where part of this work was performed, and acknowledges financial support from the Generalitat Valenciana. This work has been partially supported by DGYCIT contract No.PB 96-0753.

References

[1] C. Wilkin, nucl-th/9810047; V. Bernard, N. Kaiser, U. G. Meissner, nucl-th/9806013; J. Haidenbauer, C. Hanhart, J. Speth, Acta Phys. Polon. B 27 (1996) 2893.

[2] T. Johansson, Nucl. Phys. A 631 (1998) 331c; H. O. Meyer, Acta Phys. Polon. B 26 (1995) 553; H. Machner et al., Acta Phys. Polon. B 24 (1994) 1555.

[3] V. Bernard, N. Kaiser, U. G. Meissner, Int. J. Mod. Phys. E 4 (1995) 193.

[4] J. A. Gómez Tejedor, F. Cano, E. Oset, Phys. Lett. B 379 (1996) 39.

[5] D. M. Manley, E. M. Saleski, Phys. Rev. D 45 (1992) 4002; O. Jaekel et al., Nucl. Phys. A 511 (1990) 733.

[6] V. Sossi et al., Nucl. Phys. A 548 (1992) 562; E. Oset, M. J. Vicente Vacas, Nucl. Phys. A 446 (1985) 584.

[7] T. S. Jensen, A. F. Miranda, Phys. Rev. C 55 (1997) 1039.

[8] A. Abashian, N. E. Booth, K. M. Crowe, Phys. Rev. Lett. 5 (1960) 258

[9] F. Plouin et al., Nucl. Phys. A 302 (1978) 413.

[10] J. Banaigs et al., Nucl. Phys. B 105 (1976) 52.

[11] F. Plouin, P. Fleury, C. Wilkin, Phys. Rev. Lett. 65 (1990) 690.

[12] A. Gardestig, G. Faldt, C. Wilkin, Phys. Lett. B 421 (1998) 41

[13] L. Alvarez-Ruso, E. Oset, E. Hernández, Nucl. Phys. A 633 (1998) 519.

[14] C. L. Hollas et al., Phys. Rev. C 25 (1982) 2614.

[15] C. Anjos, D. Levy, A. Santoro, Nuovo Cimento 33 A (1976) 23.

[16] I. Bar-Nir, T. Risser, M. D. Shuster, Nucl. Phys. B 87 (1975) 109.

[17] S. Bavink et al, Nucl. Phys. A 631 (1998) 542c; http://merlin.iskp.uni-bonn.de/momo/momo.html.

[18] M. Lacombe et al., Phys. Lett. B 101 (1981) 139.

[19] R. Machleidt, K. Holinde, C. Elster, Phys. Rep. 149 (1987) 1.

[20] L. Hulthen, M. Sugawara, Handbuch der Physik, vol. 39 (Springer Verlag, Berlin, 1957).

[21] T. Ericson, W. Weise, Pions and Nuclei (Clarendon Press, Oxford, 1988), p. 25.

[22] C. Caso et al., Eur. Phys. J C 3 (1998) 1.

[23] V. Bernard, N. Kaiser, U. G. Meissner, Nucl. Phys. B 457 (1995) 147.

[24] E. Oset et al., Proceedings of the Fourth CEBAF/INT Workshop on N^* resonances (World Scientific, 1996).

[25] E. Oset, W. Weise, Nucl. Phys. A 319 (1979) 477.

[26] S. Hirenzaki, P. Fernández de Córdoba, E. Oset, Phys. Rev. C 53 (1996) 277.

[27] F. Bellemann et al., COSY Research Report 1997; C. Wilkin, private communication.

Figures

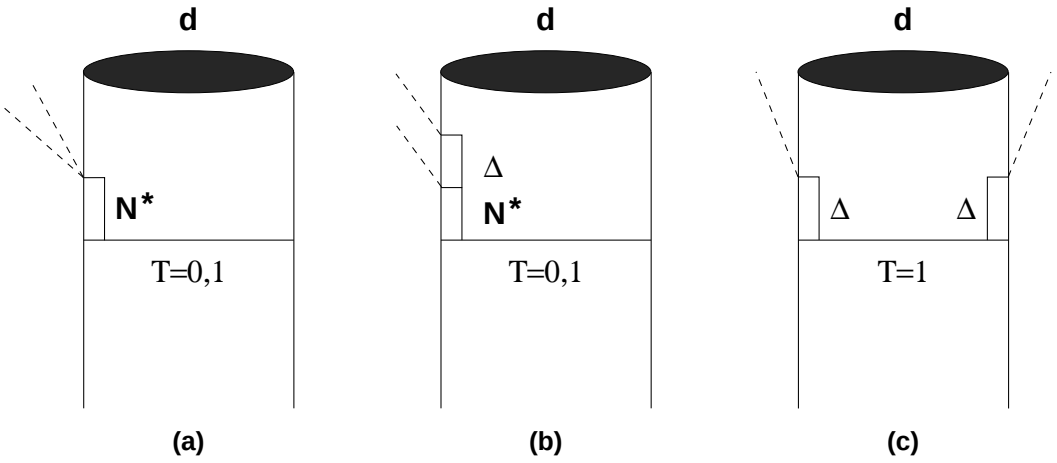

Fig. 1. Set of diagrams of the model.

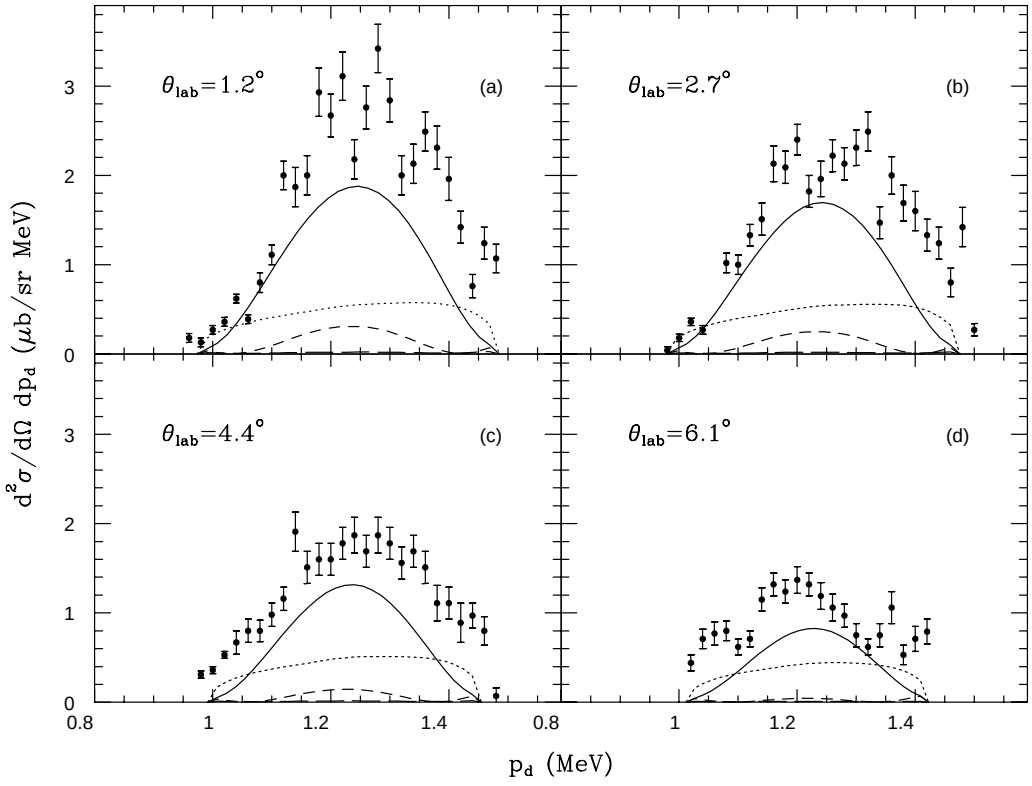

Fig. 2. Deuteron momentum spectra for $np \to d(\pi\pi)^0$ at $p_n = 1.46$ GeV and different laboratory angles (solid lines) compared to the measured data [14]. The dotted line corresponds to the $N^* \to N(\pi\pi)^{T=0}_{S-wave}$ mechanism (Fig. 1 a); the short-dashed line stands for the $N^* \to \Delta\pi$ (Fig. 1 b) and the long-dashed one, for the double-Δ (Fig. 1 c).

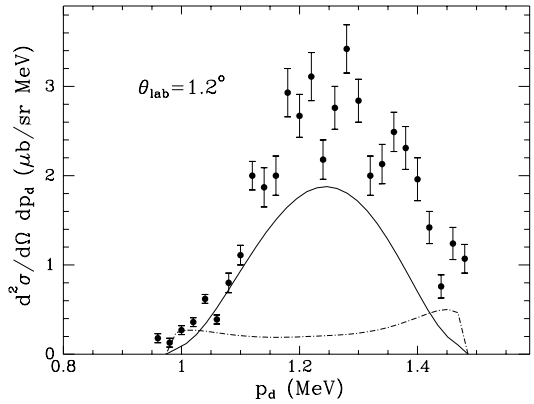

Fig. 3. Calculated spectra for two different choices of the $g_{N^*\Delta\pi}$ sign. The data clearly favor the positive sign (solid line) with respect to the negative (dash-dotted line).

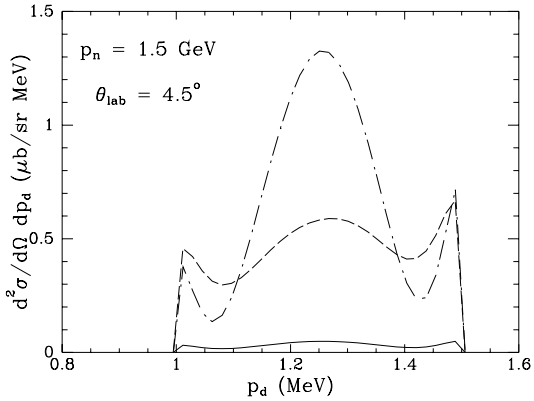

Fig. 4. Contribution of the double-Δ mechanism in the case of π exchange alone (dashed line), $\pi + \rho$ exchange (dash-dotted line) and $\pi + \rho +$ short range correlations (solid line). In this case the calculation uses a Hulthen wave function for the deuteron.

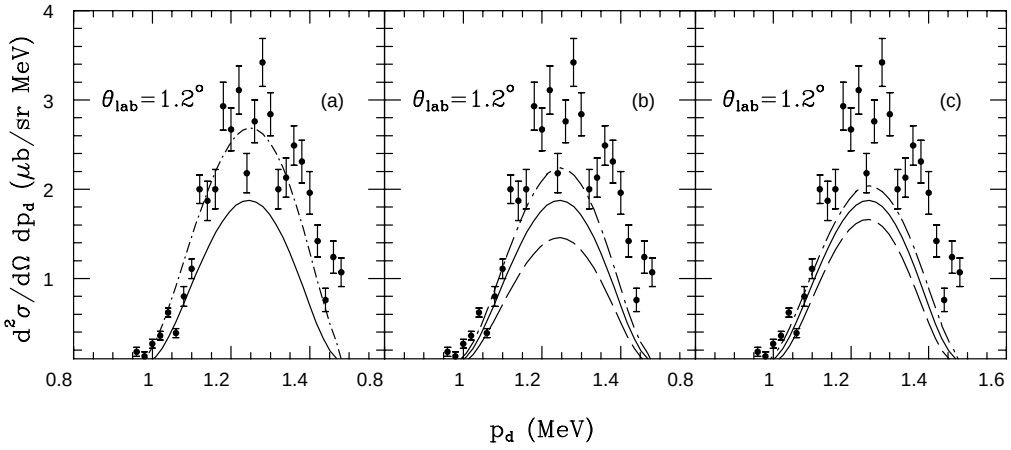

Fig. 5. Dependence of the spectrum on certain decay properties of the $N^*(1440)$. The solid line in (a) shows the result for the Set I of parameters c_1^*, c_2^* used everywhere else ($c_1^* = 0$), and the dash-dotted one is obtained for Set II. In Fig. (b), different values of the N^* total width are considered: dashed line, 250 MeV; solid line, 350 MeV; dash-dotted line, 450 MeV. The branching ratios of the different decay channels of the N^* are modified in (c), with the total width fixed to 350 MeV; dashed line: $Br(N(\pi\pi)^{T=0}_{S-wave}) = 5\%$ and $Br(\Delta\pi) = 30\%$; solid line: 7.5% and 25%; dash-dotted line: 10% and 20%.

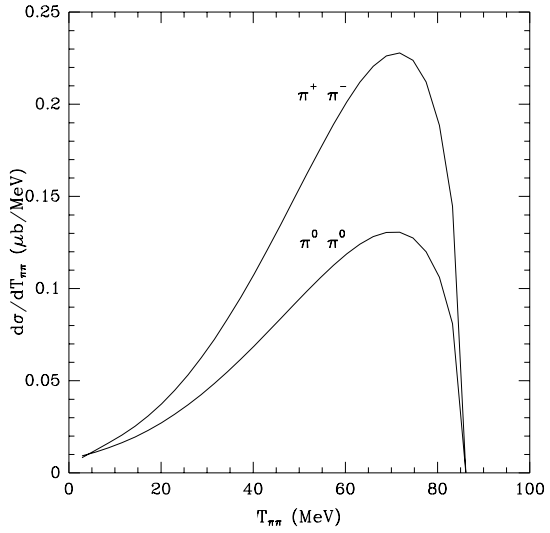

Fig. 6. Two-pion invariant mass spectrum for $np \to d\pi\pi$ at $p_n = 1460$ MeV for both charged and neutral pions.